ELSEVIER

Thermochimica Acta 387 (2002) 121–130

thermochimica acta

www.elsevier.com/locate/tca

Influence of the size of extraframework monovalent cations in X-type zeolite on their thermal behavior

U.D. Joshi[b], P.N. Joshi[a], S.S. Tamhankar[a], V.P. Joshi[c], B.B. Idage[c], V.V. Joshi[d], V.P. Shiralkar[a,*]

[a]*Catalysis Division, National Chemical Laboratory, Pashan, Pune 411 008, India*
[b]*Netaji SubhashChandra Bose College, Nanded 431 601, India*
[c]*Polymer Chemistry Division, National Chemical Laboratory, Pune 411 008, India*
[d]*Science College, Nanded 431 601, India*

Received 24 June 2001; received in revised form 2 November 2001; accepted 8 November 2001

Abstract

Pure and well crystalline NaX zeolite with Si/Al = 1.5 was prepared by hydrothermal crystallization from the Na_2O–Al_2O_3–SiO_2–H_2O system. The hydrothermal crystallization was carried out under autogeneous pressure and at static condition at 368 K. The post-synthesis modification was achieved by following conventional ion-exchange technique to obtain K^+, Rb^+ and Cs^+-exchanged forms of NaX zeolite. Compositional and structural investigations of parent sample and the samples with nearly equal population of cations with different sizes were performed by independent methods such as chemical analysis, IR, SEM, powder XRD, low temperature nitrogen adsorption. Thermal analyses data for these samples were obtained by TG/DTG/DTA and employed to evaluate the water desorption behavior. The dehydration of zeolite-type X and its modified forms was found to follow the first-order kinetics irrespective of the size of monovalent extraframework cations. Depending upon the size of extraframework cations, activation energy was found to vary from 25.4 to 27.3 kJ mol^{-1}. Enthalpy change (ΔH) values for dehydration process calculated from differential scanning calorimetric (DSC) data was found to follow the sequence NaX < NaKX < NaRbX < NaCsX in the range of 630–685 J g^{-1}. The thermal stability of these samples was found to depend on their basic character.

Keywords: Zeolite X; Alkali metal cation exchange; Thermogravimetry; Differential scanning calorimetry; Enthalpy; Thermal stability

1. Introduction

Over the past few decades, zeolites have shown [1,2] great potential for a number of applications in various fields such as adsorption, separation, ion exchange and catalysis due to their peculiar structural characteristics like: (1) three-dimensional lattice having uniform pores of molecular dimensions; (2) high internal surface area; (3) high ion-exchange capacity and (4) remarkable thermal and hydrothermal stability. The post-synthesis modification of zeolite by ion exchange is one of the approaches to tune the physico-chemical properties that are favorable for a particular application.

Zeolite of type X has a tremendous potential [3] in adsorptive, ion exchange and catalytic applications. The zeolite X, an aluminum-rich end member of faujasite

* Corresponding author. Tel.: +91-20-5890976; fax: +91-20-5890976.
E-mail address: vps@cata.ncl.res.in (V.P. Shiralkar).

0040-6031/02/$ – see front matter
PII: S0040-6031(01)00840-1

family possesses a comparatively large number of exchangeable cations and a higher framework charge. The structural arrangement of the framework cations and population of nonframework cations in different sites with/without univalent ion exchanged forms of zeolite X have been well documented [4–11]. The mobile nonframework cations are located in cavities in the channel walls and coordinated with the water molecules within the channel [12].

Earlier calorimetric [13] and infrared spectroscopy [14–18] studies on water adsorbed by alkali metal exchanged X-type zeolites have shown that a wave-like dependence exists between the heat of adsorption and the amount of water adsorbed. This suggests that water molecules present in the zeolites possess several association states of different energies. Until recently, only scarce attention has been paid to investigate the water desorption from X-type zeolites containing equal amount of monovalent extraframework cations with different sizes by thermoanalytical techniques. It was therefore thought interesting to investigate the water desorption mechanism, order and activation energy of dehydration reaction and thermal stability as a function of size of monovalent extraframework cations in X-type zeolites using thermoanalytical techniques. Other techniques such as chemical analysis, IR, SEM, powder XRD, and low temperature nitrogen adsorption were used for physico-chemical characterization of the samples.

2. Experimental

2.1. Materials

Zeolite NaX was synthesized from sodium aluminosilicate gel having the oxide mole ratios: $SiO_2/Al_2O_3 = 3.0$, $Na_2O/H_2O = 0.025$ and $Na_2O/SiO_2 = 1.2$ by hydrothermal crystallization at 368 K for 8 h. The solid product was recovered by suction filtration and washed several times with hot water to remove excess alkali. The product was then dried in an air at 383 K for 8 h. The post-synthesis modification of NaX was carried out by conventional ion-exchange technique, using 5 wt.% of aqueous solutions of K-, Rb- and Cs-chloride salts. The aqueous salt solution was taken in the proportion of 15 ml g^{-1} of zeolite, for each exchange experiment. The higher degree of exchange was achieved by repeating the cation exchange treatments at 368 K. The solid was separated by suction filtration and then washed with distilled water until the wash water is free from chloride. The solid was then dried in an air oven maintained at 383 K for 8 h. From the various modified forms, three samples were selected on the basis of almost identical degree (55.5 ± 2.5) of exchange by K^+, Rb^+ and Cs^+ cations.

The parent NaX and other three selected alkali metal exchanged zeolite X samples were moisture equilibrated over saturated solution of NH_4Cl in closed desiccator prior to the any further investigations.

2.2. Apparatus and measurements

The phase purity and crystallinity of the as-synthesized and exchanged forms were examined by powder X-ray diffraction. The powder XRD patterns were collected over 2θ range of 5–40° using Ni filtered Cu Kα ($\lambda = 1.54041$ Å) radiation using a Rigaku D Max-III VC X-ray diffractometer.

The chemical composition of parent and exchanged samples was determined by following the procedure described elsewhere [19]. In case of exchanged samples, the amount of sodium was also estimated by atomic absorption spectrometer from the filtrate collected after ion-exchanged treatment to confirm the degree of exchange.

Surface area measurements were carried out by low temperature (78 K) nitrogen sorption using a BET volumetric apparatus following the procedure describe earlier [20].

The thermal analyses DSC and TGA were carried out using Perkin-Elmer DSC-7 and Perkin-Elmer TGA-7 thermogravimetric analyzer under the nitrogen purge. The reported DSC plots were registered in dynamic N_2 flow (20 cm^3 min^{-1}) at the heating rate of 10 K min^{-1} and about 5 mg sample was taken in 50 μl sealed aluminum capsules as sample containers. The DSC base line was run from 323 to 573 K under the same condition. The DSC equipment was calibrated using indium as a reference material with an observed transition temperature 429.55 K and enthalpy change 28.43 J g^{-1}. DTA curves were recorded in air atmosphere at the heating rate of 10 K min^{-1} (model Setaram TG/DTA-92) using preheated and finely powdered α-alumina as a reference material.

Framework IR spectra of all the samples were recorded on a Pye-Unicam SP-300 spectrometer using a Nujol as a dispersing medium and polystyrene as a reference material.

The crystallite size and morphology of all the samples under investigation were examined by scanning electron microscope (model JEOL, JSM-5200, Japan). The samples were sputtered with gold to prevent surface charging and to protect them from thermal damage by the electron beam.

3. Results and discussion

3.1. Physico-chemical characteristics

The powder XRD profiles of parent and modified samples essentially showed all the characteristic peaks closely matching with the reported [21]. The absence of impurity peak(s) and amorphous halo [22] region indicated highly pure and crystalline nature of all the phases under investigation. Upon modification by conventional ion exchange, the relative intensity of the characteristic peaks was found to change without any shift in the respective peak positions. An alteration in the scattering power of X-rays due to the variation in the charge-to-size ratio of extraframework cationic species and framework distortion to some extent seems to be responsible for such observed changes in the relative intensities.

The details regarding designations, compositional and textural characteristics of the samples investigated in the present studies are summarized in Table 1. The number of exchanged extraframework cations determined by chemical analysis was found to be in close agreement with the number of sodium cations determined from the effluent collected after ion exchange followed by washing. Similarly, the framework composition (represented by square bracket in Table 1) of all the modified samples showed a close resemblance with that of the parent sample. It is seen from Table 1 that, depending on the nature and concentration of the exchanged cations, the number of unit cell per gram was found to vary in the range of 3.13×10^{19}–4.46×10^{19}. The number of unit cells per gram in exchanged forms was found to decrease with the increase in the size of exchanged cations. Table 1 also includes the intermediate electronegativity (S_{int}) of each sample and the partial charge on the oxygen atom (δ_O) evaluated using Sanderson's electronegativity equalization principle [23]. It is clearly evident from the values of S_{int} and δ_O that, these values changes as the size of extraframework cations changes in samples with isostructural features. Increase in the size of the monovalent extraframework cations seems to be operative in (i) lowering the intermediate electronegativity of the material and (ii) increasing the mean charge on the framework oxygen. Thus, when the framework negative charge is compensated by cations with low electronegativity, the charge on the framework oxygen increases which in turn increases the intrinsic framework basicity.

Low temperature nitrogen adsorption data were analyzed to estimate the specific surface area and micropore volume by applying the conventional BET and Dubinin–Radushkevich equations. It is clearly evident from Table 1 that, both the BET surface area and micropore volume decrease with the increase in the cationic size of exchanged cation. However, no linear corelationship between the difference in the kinetic diameter of the exchanged cations and corresponding increase or decrease in the values both the BET surface area and micropore volume has been observed.

Table 1
Compositional and textural characteristics of parent and cation exchanged X-type zeolites

Sample designation	Unit cell composition (on anhydrous basis)	Unit cells per gram ($\times 10^{-19}$)	Intermediate electronegativity (S_{int})	Mean charge on oxygen atom (δ_O)	BET surface area ($m^2\ g^{-1}$)	Micropore volume ($ml\ g^{-1}$)
NaX	$Na_{89.4}[(AlO_2)_{89.4}(SiO_2)_{102.6}]$	4.46	3.230	0.417	925 ± 27	0.350 ± 0.010
KNaX	$K_{47.38}Na_{42.02}[(AlO_2)_{89.4}(SiO_2)_{102.6}]$	4.22	3.115	0.441	834 ± 25	0.321 ± 0.009
RbNaX	$Rb_{47.38}Na_{42.02}[(AlO_2)_{89.4}(SiO_2)_{102.6}]$	3.66	3.081	0.448	721 ± 22	0.280 ± 0.008
CsNaX	$Cs_{51.85}Na_{37.55}[(AlO_2)_{89.4}(SiO_2)_{102.6}]$	3.13	3.008	0.464	587 ± 17	0.230 ± 0.007

The mid-infrared region of the framework IR spectra (200–1300 cm^{-1}) is useful to provide structural information as it contains the fundamental vibrations of the $Si(Al)O_4$ groupings. The obtained IR spectrum of parent sample is in close agreement with the reported literature [24]. The framework IR spectra of the modified samples revealed no shift to higher frequency in the band at 974 and 673 cm^{-1}, assigned [24] to stretching modes, which are sensitive to framework Si/Al composition. Thus, it seems that no dealumination has occurred during the ion-exchange procedure. It was, therefore, concluded that framework composition (Si/Al ratio) remained unaltered during the cation exchange process followed in the present studies. Chemical analyses data also support this conclusion.

The SEM photographs of the parent and all the modified forms have shown the crystallites of 2–3 μm size and nearly of spherical shape.

The results of powder XRD, framework IR, chemical analysis and SEM clearly indicate that the modification by ion-exchange technique has not resulted in any change as far as framework composition (Si/Al ratio), phase purity, crystallinity and crystallite size of parent NaX and its exchange forms are concerned.

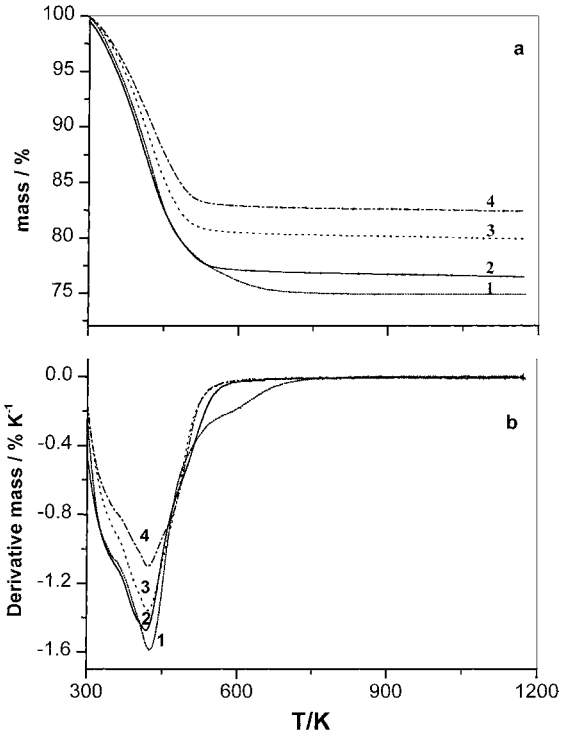

Fig. 1. (a) TG and (b) DTG thermograms of: (1) NaX; (2) NaKX; (3) NaRbX and (4) NaCsX recorded at a heating rate of 10 K min^{-1} under nitrogen atmosphere.

3.2. Thermal behavior

Thermoanalytical techniques have been found to [25,26] yield information on the mechanism as well as the thermal behavior of zeolites. In the present studies, an attempt was made to investigate the thermal properties of samples with different chemical composition having the same structural features using thermoanalytical techniques such as TG/DTG, DTA and DSC. Typical TG and DTG thermograms for the parent NaX and its exchanged forms KNaX, RbNaX and CsNaX in the temperature range of 300–1200 K are shown in Fig. 1(a) and (b), respectively. TG curves of all the samples show smooth mass loss and are devoid of any distinct steps. The striking feature of these curves is that desorption of water starts at the same temperature whereas the completion occurs at different temperatures for different samples. Generally, the zeolites undergo endothermic changes between 300 and 700 K, due to desorption of zeolitic water [27]. It can be seen from Fig. 1 that the dehydration was complete at 700 K in case of NaX, whereas at 607, 583 and 574 K for KNaX, RbNaX and CsNaX samples, respectively. Thus, the temperature required for complete desorption of water decreases with the increase in the size of nonframework cations. This can be explained on the basis of the order of regularity in the network formed by water molecules and the extent of various water molecule interactions. Water molecules are expected to interact mainly with nonframework cations, framework oxygen ions and preadsorbed water molecules [28]. However, nature of the nonframework cations is a key parameter involved in governing water–cation, water–oxygen and water–water interactions. As far as water–cation interactions are concerned, it is obvious that cations with higher electropositive character will interact more strongly with the unshared electron pair of the H_2O oxygen atom. Therefore, greater extent of water interaction is expected in case of NaX as compared to the rest of samples. It is also clear from Table 1 that; cation with less electropositive character seems to be operative in

Table 2
Quantitative estimation of micropore filling capacity using TG curves

Sample designation	Mass loss (%)	Mass loss (on anhydrous basis) (%)	Water molecules desorbed per unit cell	Micropore volume occupied by water molecules (ml g^{-1})
NaX	25.00 ± 0.5	33.33	249.9	0.333
KNaX	23.40 ± 0.5	30.55	242.16	0.305
RbNaX	19.80 ± 0.5	24.69	225.79	0.246
CsNaX	16.90 ± 0.5	20.33	217.33	0.203

enhancing the mean charge on the framework oxygen. Hence, formation of the hydrogen bond between one of the hydrogens of water molecule and nearest framework oxygen will be favored when the larger monovalent cation acts as charge balancing cation. Thus, water–oxygen interactions are favored in NaX as compared to all other modified forms. Furthermore, a reduction in the available micropore volume (as shown in Table 1) due to the exchange of larger nonframework cations may be responsible for lowering the packing efficiency of water molecules. Thus, in conclusion, the temperature required for complete desorption of water depends in the extent of various water interactions which are mainly depends on the size of nonframework cations.

The quantitative estimation of the total mass loss obtained from thermal analysis data is tabulated in Table 2. While considering the total mass loss per gram of anhydrous sample, it is of prime importance to consider number of water molecules desorbed per unit cell because the number of unit cells per gram of anhydrous sample varies depending upon the nature of nonframework cations. Therefore, the total mass loss obtained from thermal analysis data was corrected on anhydrous basis and then further treated for the estimation of the water molecules desorbed per unit cell. If amount of water molecules desorbed per unit cell was taken as a measure of hydrophilicity, following hydrophilicity trend was observed:

$$NaX > KNaX > RbNa > CsNaX$$

The extent of micropore volume occupancy by water molecules was evaluated from the amount of total water loss. It is evident from Tables 1 and 2 that, about 95% of the total micropore volume estimated from nitrogen adsorption data was occupied by water in case of NaX zeolite, whereas it is about 88% in case

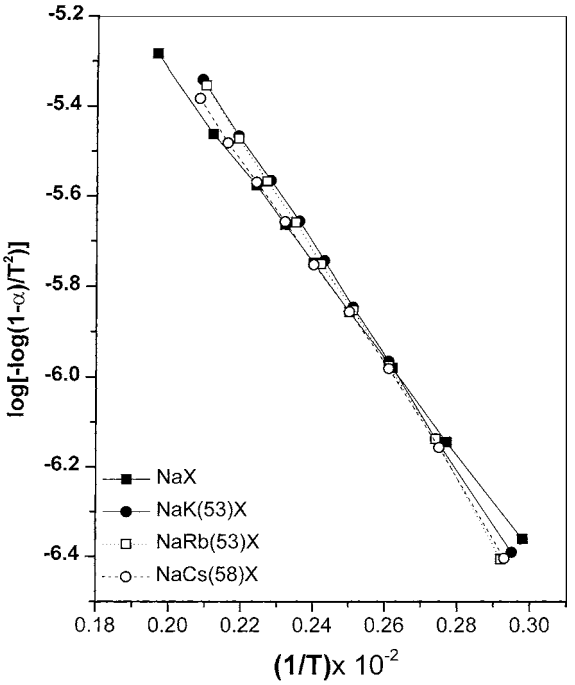

Fig. 2. Fit of experimental data for confirming the first-order dehydration process.

Table 3
Analysis of TG/DTG data and average activation energy (E_a) as a function of cationic size

Sample designation	Endothermic minima temperature, T_{min} (K)	Mass loss at T_{min} (%)	E_a (J mol^{-1})
NaX	425 ± 1	13.7 ± 0.5	25.4
NaK(53)X	422 ± 1	11.7 ± 0.5	27.0
NaRb(53)X	422 ± 1	8.9 ± 0.5	27.2
NaCs(58)X	421 ± 1	6.8 ± 0.5	27.4

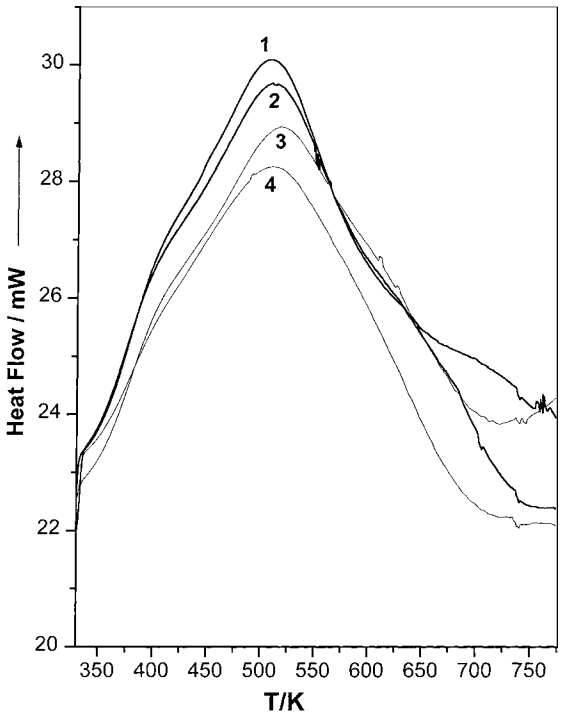

Fig. 3. DSC thermograms of: (1) NaX; (2) NaKX; (3) NaRbX and (4) NaCsX recorded at a heating rate of 10 K min^{-1} under nitrogen atmosphere.

Table 4
The DSC thermal analysis data

Sample designation	Temperature range (K)	Endothermic peak temperature, T_{max} (K)	ΔH (J g^{-1})
NaX	330–742	507 ± 1	685 ± 2
KNaX	330–745	509 ± 1	675 ± 2
RbNaX	330–747	516 ± 1	645 ± 2
CsNaX	330–750	513 ± 1	630 ± 2

of CsNaX zeolite. Thus, the size of extraframework cation was found to influence the extent of micropore volume occupancy by water molecules.

In order to investigate the energetics and the kinetics of dehydration process in samples with varying cationic size, the parameters such as activation energy and order of reaction were calculated. The process of dehydration of zeolites is reported [29,30] similar to the reaction type

$$\mathrm{A\,(solid)} \rightleftharpoons \mathrm{B\,(solid)} + \mathrm{C\,(gas)} \quad (1)$$

and is usually described by the well-known kinetic equation [29]

$$\frac{d\alpha}{dt} = [A_0\, e^{-E_a/RT}](1-\alpha)^n \quad (2)$$

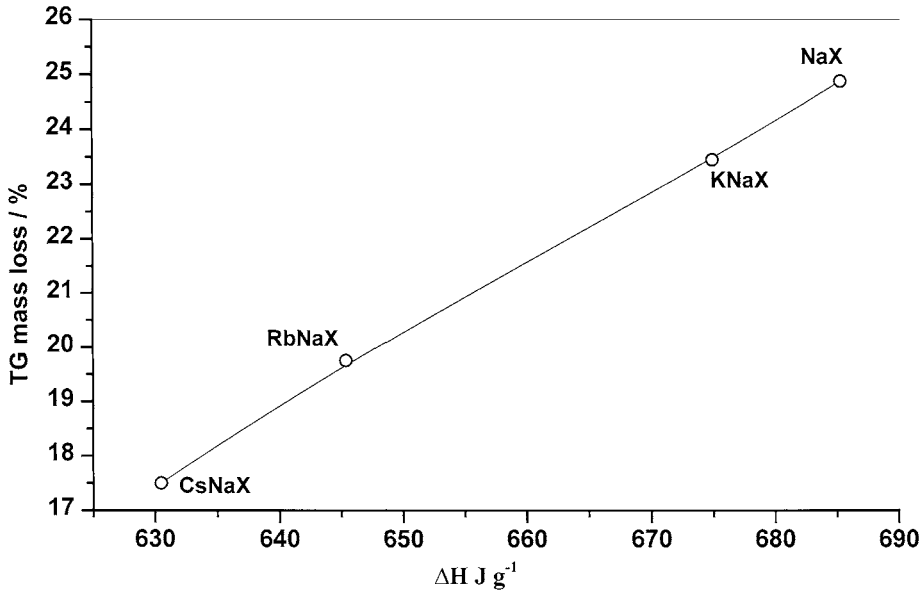

Fig. 4. The corelationship between percentage mass loss and ΔH for parent and modified forms of X-type zeolites.

where α is the degree of conversion, A_0, E_a and n are constants representing the frequency factor, activation energy and order of reaction, respectively. The value of n evaluated separately from DTA endothermic peaks using "shape index" factor (S) by Kissinger's method [29]. The calculated values of n are nearly equal to 1 (1.06 ± 0.04) which indicates that the dehydration of zeolites studied follows first-order kinetics [31]. With $n = 1$, Eq. (2) coincides with Barrer's equation [32]. The order of the reaction was also confirmed by the linearity of a plot $-\log[-\log(1-\alpha)/T^2]$ vs. $1/T$ as depicted in Fig. 2. The average activation energy values calculated by applying the Coats–Redfern equation [31] to the TG/DTG data are summarized in Table 3. The values of E_a were found to depend on the size of nonframework cations and were found to lie in the range of 6.06–6.53 kcal mol^{-1}. Furthermore, the values obtained for

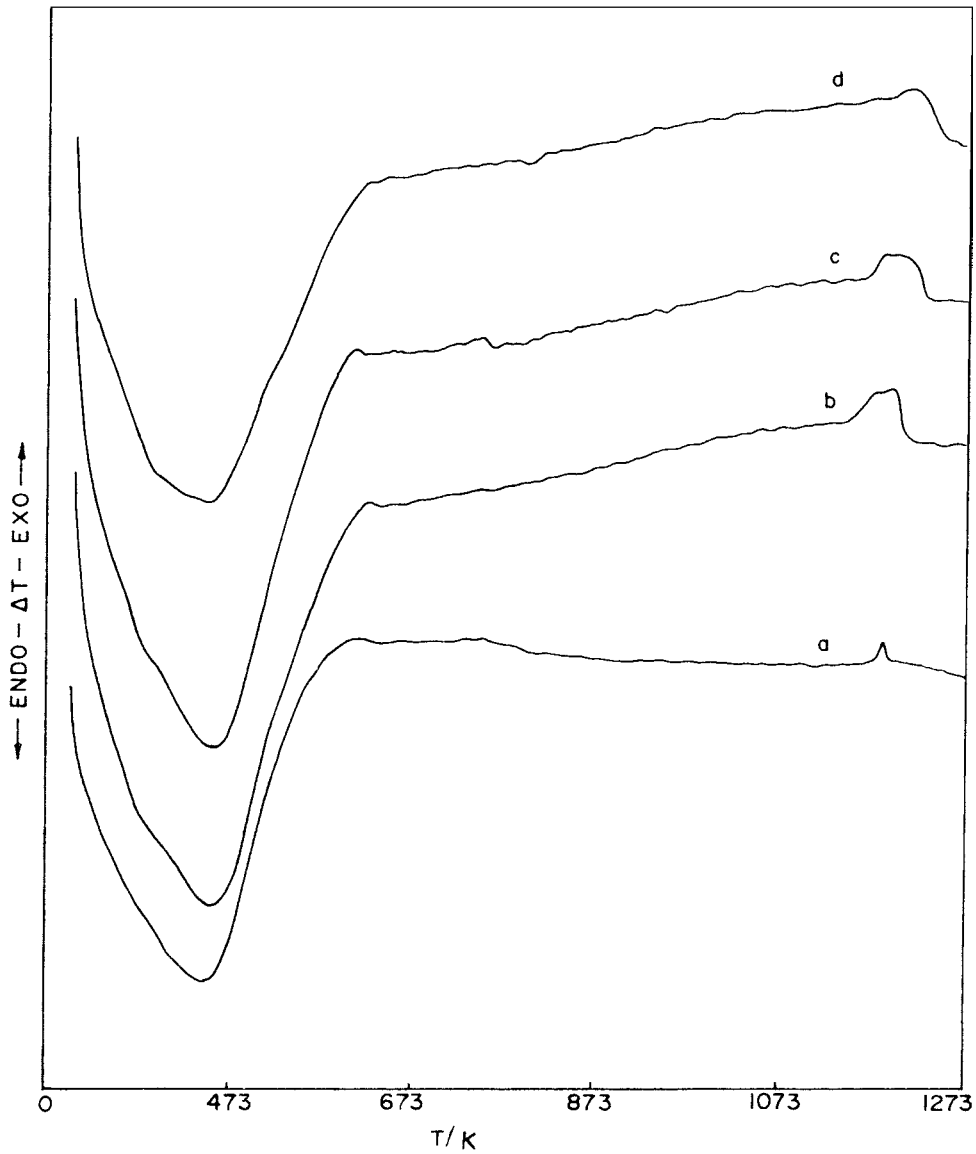

Fig. 5. DTA thermograms for: (a) NaX; (b) NaKX; (c) NaRbX and (d) NaCsX.

the minima of DTG endotherm (T_{min}) and percentage mass loss at T_{min} suggest that the rate of dehydration depends upon the nonframework cationic size. This may be attributed to the total water content in micropore volume of the zeolite and the extent of various water interactions.

In view of proven higher precision of DSC signals that exhibit identifiable peaks with high sensitivity as compared to DTA signals [33–35], the DSC technique was used to determine water desorption behavior in the present studies. The DSC thermograms were obtained for the samples used in TG analysis and are shown in Fig. 3. The figure shows that, in all the cases a large single endothermic peak due to desorption of water was obtained in the temperature range from 300 to 750 K. It is interesting to note that, eventhough zeolite Y belongs to the same class as zeolite X, protonic form of Y zeolite has shown [34] two widely separated endotherms due to water desorption from large supercage and small β-cages.

The DSC thermal analysis data for NaX and its exchanged forms are tabulated in Table 4. The water content is comparatively measured in terms of enthalpy change (ΔH). The ΔH values are evaluated using "peak integration". The obtained value of ΔH was found to be in the range of 630–685 J g^{-1}. This indicates that enthalpy change values (ΔH) also decrease with the increase in the size (i.e. decrease in charge density) of nonframework cations. The trend observed for ΔH values of the samples under study is the same as the percentage mass loss obtained from TG. It indicate that parent NaX has higher ΔH value than the K-, Rb-, Cs-exchanged forms.

Fig. 4 gives a correlation between percentage mass loss due to water desorption obtained from TG thermograms and the values ΔH obtained from DSC thermograms for water desorption. Since ΔH is related to mass [35], the linear plot obtained in the figure indicates that TG mass loss increases with the increase in ΔH. Moreover, the ratio of ΔH to TG mass loss percentage was found to increase with the increase in the nonframework cationic size indicative of dependence of the water desorption on nature and size of nonframework cations in zeolite.

Thermal stability of zeolites is an important parameter for their application in various fields. It is known [36] that thermal stability of the zeolitic framework increases with the increase in Si/Al ratio. As described in Section 3.1, all the samples investigated in the present studies have shown identical framework Si/Al ratio. Therefore, the influence of the size of nonframework cations on their thermal stability was investigated on the basis of almost identical population of different monovalent cations. The temperature of the maximum of the high temperature exotherm in DTA thermograms is often taken [37] as a criterion for the thermal stability of the zeolitic framework. Fig. 5 illustrates the DTA curves of NaX, NaKX, NaRbX and

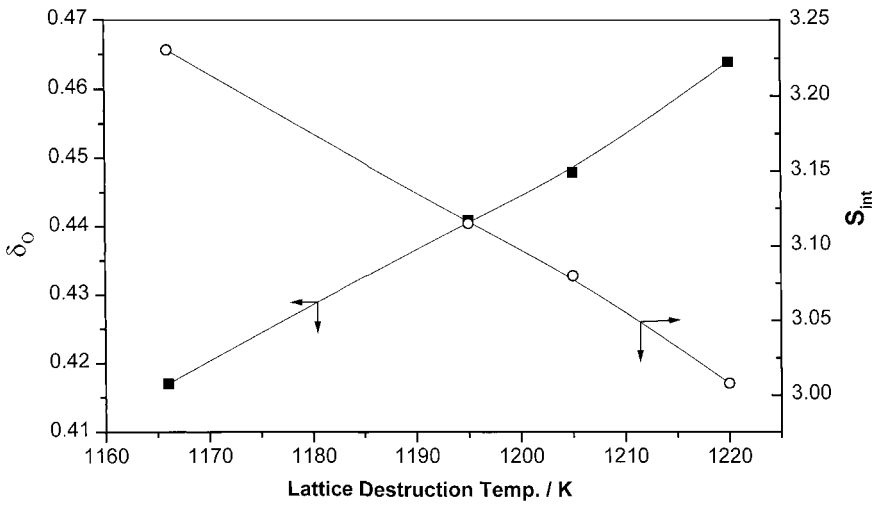

Fig. 6. Dependence of lattice destruction temperature on the intermediate electronegativity of the material and the framework oxygen charge.

NaCsX sample and it was revealed that the lattice destruction temperature for these samples occur at 1166, 1195, 1205 and 1220 K, respectively. This indicates that not only framework Si/Al ratio is responsible for the thermal stability of particular zeolite but also the size of the nonframework cations. This can be attributed to intermediate electronegativity and charge on the framework oxygen. Fig. 6 depicts the corelationship established between the lattice destruction temperature and the intermediate electronegativity and charge on the framework oxygen. It is clearly seen from the figure that, as intermediate electronegativity of the material increases, the lattice destruction temperature was found to decrease. On the contrary, the lattice destruction temperature was found to increase with the increase in the charge on framework oxygen. This can be associated with [38] the changes in the Si–O–Al bond angle and T–O distances favoring the thermal stability of the zeolitic lattice. Thus, if oxygen charge is treated as the measure of the basicity, thermal stability of zeolite was found to increase with the increase in the basic character of the zeolite.

4. Conclusions

Upon modification by ion-exchange technique, no change has been observed in the framework composition (Si/Al ratio), phase purity, crystallinity and crystallite size of parent NaX and its K^+-, Rb^+- and Cs^+-exchanged forms. However, the textural characteristics such as surface area and micropore volume evaluated from the low temperature nitrogen adsorption isotherm data showed the dependence on the size of the nonframework-exchanged cation.

The thermoanalytical data obtained from TG/DTG and DTA showed that the temperature required for complete desorption of water decreases with increase in the size of nonframework cations. This can be explained on the basis of the order of regularity in the network formed by water molecules and the extent of various water molecule interactions. The process of dehydration in all the forms have shown follow first-order kinetics indicating the independence of size of nonframework cations on the order of dehydration process in the present studies. Thermal stability of zeolite was found to increase with the increase in the basic character of the zeolite on account of the presence of larger and less electropositive nonframework monovalent cation. The average activation energy E_a was found to vary in the range of 25.4 for parent NaX zeolite to 27.3 kJ mol^{-1} for its exchanged forms. The obtained value of ΔH was found to be in the range of 630–685 J g^{-1} for these samples. Nearly linear correlation was observed between ΔH and percentage mass loss of water from zeolitic samples.

Acknowledgements

U.D.J. and V.V.J. express their thanks to Dr. Paul Ratnasamy, Director of the National Chemical Laboratory, Pune, for permission to carryout the research work. U.D.J. thanks to UGC and the Vice Chancellor of the Swami Ramanand Teerth Marathwada University, Nanded for availing FIP scheme.

References

[1] H.V. Bekkum, E.M. Flanigen, J.C. Jansen (Eds.), Introduction to Zeolite Science and Practice, Elsevier, Amsterdam, 1991.
[2] R.L. Mays, P.E. Pickert, Molecular Sieves, Soc. Chem. Ind., London, 1968, p. 112.
[3] S.P. Zhdanov, S.S. Khvoshchev, N.N. Feoktistova, Synthesic Zeolites, Vol. II, Institute of Silicate Chemistry, USSR Academy of Science, Leningrad, 1990.
[4] D.H. Olson, Zeolites 15 (1995) 439.
[5] D.H. Olson, J. Phys. Chem. 74 (1970) 2758.
[6] H. Breamer, W. Wörke, R. Schödel, F. Vogt, in: W.H. Meier, J.B. Uytterhoeven (Eds.), Molecular Sieves: Advanced Chemical Series, Vol. 121, American Chemical Society, Washington, DC, 1973, p. 249.
[7] H.S. Sherry, J. Phys. Chem. 70 (1996) 1158.
[8] W.J. Mortior, H.J. Bosmons, J.B. Uytterhoeven, J. Phys. Chem. 76 (1972) 650.
[9] N.U.T. Shepelev, I.K. Butikova, Yu. Smolin, Zeolites 11 (1991) 287.
[10] Yu.E. Shepelev, A.A. Anderson, Yu. Smolin, Zeolites 10 (1990) 61.
[11] C. Farano, R.C.T. Slade, I.G. Krogh Adersen, E.J. Price, J. Solid State Chem. 82 (1989) 95.
[12] D.W. Breck, Zeolite Molecular Sieves, Wiley, New York, 1974, p. 397.
[13] O.M. Dzhigit, A.V. Kiselev, K.N. Mikos, G.G. Muttik, T.A. Rahmanova, Trans. Faraday Soc. 67 (1971) 458.
[14] L. Bertsch, H.W. Habgood, J. Phys. Chem. 67 (1963) 1621.
[15] J.W. Ward, J. Phys. Chem. 72 (1968) 4211.
[16] J.B. Uytterchoeven, R. Schoonheydt, J. Catal. 13 (1969) 425.
[17] R.C. Hansford, J.W. Ward, Adv. Chem. Ser. 102 (1971) 354.

[18] A.V. Kiselev, V.I. Lygin, Infrared Spectra of Surface Compounds and Adsorbed Substances, Nauka Moscow, Russia, 1972.
[19] U.D. Joshi, P.N. Joshi, S.S. Tamhankar, V.V. Joshi, V.P. Shiralkar, J. Colloid Interf. Sci. 235 (2001) 135.
[20] V.P. Shiralkar, Ph.D. Thesis, University of Pune, 1980.
[21] D.W. Breck, Zeolite Molecular Sieves, Wiley, New York, 1974.
[22] P.N. Joshi, T.H. Kim, K.I. Kim, V.P. Shiralkar, Adsorp. Sci. Technol 17 (8) (1999) 639.
[23] R.T. Sanderson, Chemical Bonds and Bond Energy, Academic Press, New York, 1976.
[24] E.M. Flanigen, H. Khatami, H.A Szymanski, in: R.F. Gould (Ed.), Molecular Sieve Zeolites. I. Advance Chemical Series, Vol. 101, American Chemical Society, Washington, DC, 1971, p. 201.
[25] E.G. Derouane, S. Detremmerie, Z. Gabelica, N. Blom, Appl. Catal. 1 (1981) 201.
[26] R.M. Barrer, D.V. Langely, J. Chem. Soc. (1958) 3804, 3811, 1817.
[27] V.P. Shiralkar, S.B. Kulkarni, J. Therm. Anal. 25 (1982) 399.
[28] A.V. Kiselev, I.V. Lygin, R.V. Starodubceva, Chem. Soc., Faraday Trans. 1 68 (1972) 1793.
[29] H.E. Kissinger, Anal. Chem. 29 (1957) 1702.
[30] G.O. Piloyan, O.S. Novikova, Inorg. Mater. 2 (1966) 1109.
[31] A.W. Coats, J.P. Redfern, Nature 201 (1964) 68.
[32] R.M. Barrer, G.C. Bratt, J. Phys. Chem. Solids 12 (1959) 130, 146.
[33] A.K. Aboul-Gheit, M.A. Al-Hajjaji, A.M. Summan, S.M. Abdel-Hamid, Thermochim. Acta 126 (1988) 397.
[34] A.K. Aboul-Gheit, Thermochim. Acta 160 (1990) 193.
[35] A.K. Aboul-Gheit, M.A. Al-Hajjaji, Anal. Lett. 20 (1987) 553.
[36] D.W. Breck, Zeolite Molecular Sieves, Wiley, New York, 1974, p. 449.
[37] H. Bremer, W. Morke, R. Schodel, F. Vogt. Adv. Chem. Ser. 121 (1973) 249.
[38] G.V. Gibbs, E.P. Meagher, J.V. Smith, J.J. Pluth, ACS Symp. Ser. 40 (1977) 19.